E6-2004-7

YIELD OF RADIONUCLIDES AND ISOMERS MEASURED IN FRAGMENTATION OF THE ^{nat}W AND ^{186}W (97%) TARGETS WITH PROTONS AT 630, 420 AND 270 MeV

Submitted to «Nuclear Instruments and Methods A»

S. A. Karamian[1*], J. Adam[1,2], P. Chaloun[1,2], D. V. Filossofov[1], V. Henzl[2,3], D. Henzlova[2,3], V. G. Kalinnikov[1], N. A. Korolev[1], N. A. Lebedev[1], A. F. Novgorodov[1], C. B. Collins[4], I. I. Popescu[5], C. A. Ur[5]

[1]Joint Institute for Nuclear Research, Moscow region, 141980, Dubna, Russia
[2]Nuclear Physics Institute, Rez, Prague CZ-25068, Czech Republic
[3]Gesellschaft für Schwerionenforschung, D-64291, Darmstadt, Germany
[4]Center for Quantum Electronics, University of Texas at Dallas, Dallas, TX 75083, USA
[5]National Institute of Physics and Nuclear Engineering
and Induced Gamma Emission Foundation, Bucharest 76900, Romania
*E-mail address: karamian@nrmail.jinr.ru

Карамян С. А. и др. Е6-2004-7
Выход радиоизотопов и изомеров при фрагментации мишеней из ^{nat}W и ^{186}W (97 %) протонами с энергией 630, 420 и 270 МэВ

Выходы и сечения образования радиоактивных ядер измерены по γ-активности после облучения мишеней из W естественного изотопного состава и обогащенного ^{186}W на пучке синхроциклотрона в Дубне. Среди обнаруженных ядер представлены продукты реакций скалывания и деления. Получены высокоспиновые изомеры Hf и Lu и определены соответствующие изомерные отношения. Выходы ядер также рассчитаны с использованием кода LAHET при 6 значениях энергии протонов от 100 до 800 МэВ как для мишени из ^{nat}W, так и для ^{186}W. Измеренный выход изотопов, в общем, согласуется с расчетом, однако изомерные отношения не предсказываются в пределах использованного метода расчета. В мишени из обогащенного ^{186}W (97 %) высокоспиновые изомеры ^{177m}Lu, ^{178m2}Hf и ^{179m2}Hf получаются с более высоким выходом (в 2,5 раза), чем в мишени из ^{nat}W при тех же условиях облучения. Это важно для создания изомерных источников излучения высокой активности. Получены и сравниваются с теорией массовые распределения продуктов реакции и отношения полных сечений деления и скалывания.

Работа выполнена в Лаборатории ядерных реакций им. Г. Н. Флерова и в Лаборатории ядерных проблем им. В. П. Джелепова ОИЯИ.

Препринт Объединенного института ядерных исследований. Дубна, 2004

Karamian S. A. et al. E6-2004-7
Yield of Radionuclides and Isomers Measured in Fragmentation of the ^{nat}W and ^{186}W (97%) Targets with Protons at 630, 420 and 270 MeV

Yields and cross sections of the radioactive nuclide formation have been measured via induced activity γ-spectra after irradiation of the natural composition W and enriched ^{186}W targets at Dubna synchrocyclotron. Spallation and fission products have been represented among the detected nuclides. The high-spin isomers of Hf and Lu were produced and the isomer-to-ground state ratios could be estimated. The nuclide yields have also been calculated using the LAHET code at 6 values of proton energy in the range from 100 to 800 MeV both for ^{nat}W and for enriched ^{186}W targets. Measured isotope yields are generally in agreement with the calculations, however, the code is incapable to predict the isomer-to-ground state ratios. In experiment, it has been shown that the ^{177m}Lu, ^{178m2}Hf and ^{179m2}Hf high-spin isomers are produced with 2.5 times higher yield in the 97% enriched ^{186}W target as compared to the ^{nat}W target at identical irradiations. This makes significance for the creation of high-activity isomeric sources. The mass-distribution of products and fission-to-spallation ratio are also deduced and are compared with the theory prediction.

The investigation has been performed at the Flerov Laboratory of Nuclear Reactions and at the Dzhelepov Laboratory of Nuclear Problems, JINR.

Preprint of the Joint Institute for Nuclear Research. Dubna, 2004

INTRODUCTION

Studies in the field of high-spin nuclear isomers are important both for nuclear structure science and for innovating applications. The triggered release of the energy stored in nuclear isomers is promising for the creation of pulsed sources of gamma-radiation. Specific energy stored by some isomers for long period of time is much higher as compared to the standard sources of energy. For instance, the high-spin $K^{\pi} = 16^{+}$ ^{178m2}Hf isomeric state stores a specific energy of about 1.3 MJ/mg with a half-life of 31 years. For applicative purposes and extensive studies on the trigger mechanisms one needs to produce isomers in quantities of milligrams, or even more, in extreme. Our study is part of the efforts to use spallation reactions with protons of intermediate energies as a source for high-spin nuclear isomers production.

In the previous study we investigated the production of the high-spin isomers of Hf and Lu isotopes at spallation of natural Ta and Re targets [1]. The results on the isomer yields, the isomer-to-ground state ratios, mass distributions of the spallation products and the fission-to-spallation ratios were extracted and compared with the theory predictions. It was established that the yield of the ^{178m2}Hf isomers is limited mainly because of two reasons: a) a high value of the isomeric-state spin results in a reduction of the isomer-to-ground state ratio and b) the location of ^{178}Hf near the β-stability line while the spallation products are typically neutron deficient. The production of ^{178m2}Hf can be increased by the use of targets as rich as possible in neutrons. A survey of the available isotopes in this mass region has indicated as the best candidate for the target material the ^{186}W isotope.

In the present work measured radionuclide yields (including isomers) are reported for the irradiation of a W targets, in natural composition ($^{\rm nat}$W), and isotopically enriched ^{186}W with protons at 630, 420 and 270 MeV. Spallation reactions of both $^{\rm nat}$W and enriched ^{186}W targets were simulated with the LAHET code for proton energies in the range from 100 to 800 MeV.

1. EXPERIMENT AND RESULTS

97% enriched ^{186}W material has been commercially supplied in a form of metal pieces about 1.5 mm thick. They were fixed to the Al holder with 50 μm

foil of $^{\rm nat}$W used as a support. Such construction was inserted for the irradiation into the internal beam of protons at the synchrocyclotron of DLNP, JINR Dubna, as shown schematically in Fig. 1. Heat released by the beam in the target was successfully transferred to the cooled Al backing. In synchrocyclotron (phasotron), the beam energy is roughly proportional to the radius square. The position of targets inside the accelerator was chosen in accordance with known calibrations to provide the beam energy values of 650, 450 and 300 MeV at different irradiations.

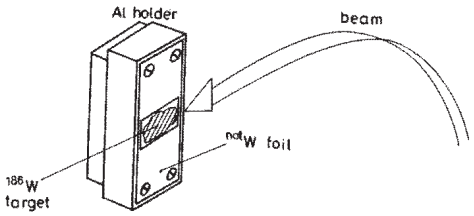

Fig. 1. Scheme of the target irradiation at the internal beam of Dubna phasotron

A 3 g amount of 97% enriched ^{186}W material was enough in order to prepare 3 targets of similar construction for the irradiation at synchrocyclotron. In such design target, the proton beam exposes at one irradiation the pieces of enriched ^{186}W material and the holder foil made of $^{\rm nat}$W. This way, we arrange simultaneous irradiation of both ^{186}W and $^{\rm nat}$W targets at identical conditions that would be important for the comparison, being economic in beam time, as well.

Gamma-spectroscopy measurements of irradiated samples have been started after "cooling" for one month because of high activity of short lived radionuclides accumulated during the activation. After series of measurements, the samples were dissolved for the chemical processing and isolation of the Hf fraction. Activity of the long-lived ^{178m2}Hf is rather low as compared to other nuclides activity, and the chemical isolation was necessary to achieve good statistical accuracy for the ^{178m2}Hf yield measurements.

The differential chromatography of elements in resin-filled columns and other radiochemical methods have been used in a multi-step chemical processing of the irradiated target material. After dissolution in concentrated acid, the crude isolation of the Hf fraction from the bulk W matter was followed by the fine rectification from remaining Re, W and rare-earth elements substances. Before the measurement, the Hf fraction was finally purified from the Lu accumulated as a daughter of Hf radionuclides decay. The latter operation was necessary for removal of the ^{172}Lu background activity and, thus, for the improved accuracy of the ^{178m2}Hf γ-lines intensity measurement.

The HP Ge detector of 20% efficiency (in ratio to the standard NaI scintillator) assembled with the compatible electronics provides a spectral resolution of 1.8 keV by ^{60}Co γ lines and moderate dead-time at high count rate up to 20 kCs/s. The geometry of measurement (the distance and absorber) has been optimized for each sample. The energy and efficiency calibration using the standard sources

allowed the linking of different measurements with good accuracy. The method of intrinsic calibration by intense γ lines of ^{172}Hf and ^{175}Hf was also applied. This way, the self-absorption factor had been determined for gammas emitted from ^{186}W samples 1.5 mm thick.

In the measured spectra, the lines belonged to as many as of about 70 radionuclides have been identified, they all are the products of the tungsten target fragmentation. A number of atoms for each nuclide could be determined using the corresponding γ-line intensity in measured spectrum, with the account of the detector efficiency, decay factor, and individual spectroscopic properties of nuclides. The latter parameters were found in "Table of Isotopes" [2], in Ref. [3], and for some cases in the "Nuclear Data Sheets" compilation. The obtained number should be recalculated to the absolute yield of a nuclide per one projectile proton and to the mean cross section, respectively.

The cross section is evaluated per one W nucleus in a target without differentiation of isotopes in the multi-isotopic target material. For consistency, the same definitions are also used in the Monte-Carlo code simulation. In the geometry of Fig. 1, a number of protons exposed the target can only be estimated by an order of magnitude. Thus, the measured values should be calibrated attracting additional information. The "LAHET" code simulations have been used for this purpose. A group of nuclides measured with the best statistical accuracy, namely ^{167}Tm, ^{169}Yb, ^{172}Hf, ^{173}Lu, ^{175}Hf and ^{183}Re, is included for deducing the calibration coefficient by comparison of the measured and calculated yields. Another option for calibration is based on the known in literature cross sections [4] for $^{\rm nat}$W target. Both variants have been applied and they show reasonable agreement. Finally, a mean value is used to get an actual calibration coefficient.

As is mentioned above, the activity of exposed targets was rather high because of massive targets and high fluences. Hence, the "cooling" for one month was necessary before measurements. Respectively, short-lived isotopes were decayed and their yield was inaccessible for the experimental definition. Some other groups, Refs. [5, 6], arrange short-time cycle for irradiation and measurement with a successful detection of the short-lived isotopes. However, our order of experimental operations has the advantage in the possibility to observe the yield of low-activity products. This was important for detection of the 31-years-lived ^{178m2}Hf isomer and other long-lived products. The low-yield nuclides were also determined, and more information on the fission yield and mass-distribution was received, as compared to [5, 6]. A total number of detected isotopes was comparable, but our set of standard products is different from that by [5, 6]. Means, present work, Ref. [1] and [5, 6] measurements provide, in principle, a supplementary results, but the choice of targets and proton energies is mainly different. That makes a direct comparison difficult.

The γ-ray spectra measured with high statistical accuracy contain both high-intensity peaks and relatively weak γ lines. The spectra are processed with the

best as possible preciseness using the "DEIMOS" software code developed in Ref. [7]. A spectrum is reproduced to reach the lowest deviations varying a number of γ lines and their position at each region of interest and applying the standard information on the peak widths from the calibration spectra. Finally, accurate values of the line energy, its' area and the statistical error were deduced for all lines found in the spectrum. The standard deviation for any individual yield value is defined by the statistical error of the corresponded γ-line area and by the systematical errors. The latter ones are arising due to the absolute calibration of the yields, the inaccuracy on the measured efficiency of detectors and the errors on the tabular standards like quantum yields of characteristic γ-ray lines belonging to the individual nuclides. The total errors vary typically from 5% for the best cases to 40% for the cases of low intensity γ-ray lines in the spectra.

The comparison of measured cross sections with calculated ones both for $^{\rm nat}$W and ^{186}W targets are given in Tables 1–3 corresponded to 3 values of the proton energy. The mean energy value is deduced with the account of energy loss in the target. Here and below, indication of "^{186}W target" corresponds to the 97% enriched target for experimental results and to 100% pure ^{186}W for calculated ones. LAHET code in the classical version [8] has been used for Monte-Carlo simulations of the product yields. The statistical accuracy of the Monte-Carlo procedure can be estimated as following. At present series of simulations one nucleus produced in the reaction corresponds to the cross section of $3{\cdot}10^{-30}$ cm^2. The individual cross section given in the tables for any product allows calculating a number of this kind nuclei appeared after simulation. Thus, the statistical accuracy is determined for the product cross section obtained in the Monte-Carlo simulation.

Table 1: **Cross section values in mbarn for the fragmentation products at 630 MeV mean proton energy with the $^{\rm nat}$W and ^{186}W (97%) targets, as measured and as predicted within the LAHET code simulations. Errors are given in brackets. Remark is valid for Tables 2 and 3, as well**

Isotope	Type of yield	^{186}W target		$^{\rm nat}$W target	
		Experiment	Calculation	Experiment	Calculation
^{184}Re	Indep.	4.5 (.2)	} 7.3	1.10 (.05)	} 2.8
^{184m}Re	Indep.	1.2 (.2)		0.26 (.04)	
^{183}Re	EC cum.	6.8 (1.0)	9.6	2.7 (.4)	5.2
^{183}Ta	β^-cum	19 (3)	–	16.0 (2.5)	–
^{182}Ta	Indep.	15.8 (1.5)	16.6	10.4 (1)	17.5
^{181}Hf	β^-cum	2.3 (.1)	2.9	0.93 (.05)	1.88
^{179m2}Hf	Indep.	0.80 (.08)	4.0	0.36 (.04)	2.86

Table 1 (Continue)

Isotope	Type of yield	^{186}W target		^{nat}W target	
		Experiment	Calculation	Experiment	Calculation
^{178}W	EC cum.	21.8 (2)	34.8	23 (2)	38.1
^{178m2}Hf	Indep.	0.48 (.07)	5.7	0.18 (.03)	4.3
^{177m}Lu	Indep.	0.26 (.05)	1.16	0.13 (.03)	0.75
^{175}Hf	EC cum.	55.6 (2.8)	57.4	55.0 (2.7)	56.9
^{174}Lu	Indep.	1.4 (.4)	} 3.16	1.3 (.4)	} 2.11
^{174m}Lu	Indep.	1.55 (.3)		1.6 (.3)	
^{173}Lu	EC cum.	60 (3)	60.5	61 (3)	58.9
^{172}Hf	EC cum.	57.4 (2.9)	50.8	53.5 (2.7)	53.8
^{171}Lu	EC cum.	60 (8)	58.2	61 (8)	58.5
^{169}Yb	EC cum.	52 (2.6)	53.5	55.0 (2.7)	55.0
^{168}Tm	Indep.	1.0 (.15)	0.85	0.73 (.11)	0.42
^{167}Tm	EC cum.	46.5 (2.3)	46.0	55.0 (2.7)	48.5
^{156}Tb	Indep.	0.27 (.05)	0.56	0.23 (.04)	0.45
^{156}Eu	β^-cum	0.12 (.04)	0.003	0.10 (.03)	–
^{155}Tb	EC cum.	18.7 (3.7)	23.1	25 (5)	26.2
^{153}Gd	EC cum.	–	17.6	10.5 (1.6)	20.3
^{151}Gd	EC cum.	8.4 (1.3)	13.0	9.6 (1.5)	15.9
^{149}Gd	EC cum.	6.9 (0.7)	9.1	10.5 (1.0)	12.4
^{149}Eu	EC cum.	7.0 (0.5)	10.2	11.0 (.8)	13.4
^{148}Eu	Indep.	0.34 (.04)	1.52	0.36 (.04)	1.27
^{148m}Pm	Indep.	0.02 (.006)	0.016	0.03 (.01)	0.009
^{147}Eu	EC cum.	3.9 (.4)	8.3	6.7 (.7)	11.6
^{146}Gd	EC cum.	3.5 (.3)	5.7	7.3 (0.6)	8.6
^{145}Eu	EC cum.	1.9 (.4)	5.6	7.0 (1.5)	7.9
^{144}Pm	Indep.	0.078 (0.031)	0.56	0.15 (.06)	0.52
^{143}Pm	EC cum.	1.13 (.17)	4.8	2.1 (.4)	6.3
^{140}Ba	β^-cum	0.002 (.001)	–	0.003 (.001)	–
^{139}Ce	EC cum.	–	–	0.67 (.22)	–
^{133}Ba	EC cum.	–	0.48	0.28 (.05)	0.68
^{131}Ba	EC cum.	0.16 (.06)	0.22	0.33 (.12)	0.44
^{126}I	Indep.	0.006 (.003)	–	0.007 (.003)	–
^{121}Te	EC cum.	0.061 (.025)	0.09	0.20 (.08)	0.068
^{113}Sn	EC cum.	0.054 (.015)	0.103	0.07 (.02)	0.111

Table 1 (Continue)

Isotope	Type of yield	^{186}W target		^{nat}W target	
		Experiment	Calculation	Experiment	Calculation
^{110m}Ag	Indep.	0.046 (.010)	0.044	0.05 (.01)	0.025
^{106m}Ag	Indep.	0.10 (.02)	0.096	0.080 (.015)	0.093
^{105}Ag	EC cum.	0.21 (.06)	0.103	0.16 (.03)	0.133
^{103}Ru	β^-cum	0.14 (.05)	0.094	0.11 (.04)	0.065
^{102}Rh	Indep.	0.13 (.03)	0.143	0.08 (.02)	0.164
^{100}Pd	β^+cum	0.056 (.01)	0.031	–	0.052
^{95m}Tc	Indep.	0.019 (.008)	–	0.03 (.01)	–
^{95}Nb	Indep.	0.14 (.02)	0.197	0.17 (.02)	0.13
^{95}Zr	β^-cum	0.050 (.01)	0.059	0.04 (.01)	0.037
^{91m}Nb	Indep.	0.021 (.006)	0.225	0.047 (.015)	0.228
^{88}Zr	EC cum.	0.19 (.02)	0.324	0.18 (.02)	0.27
^{88}Y	Indep.	0.24 (.02)	0.275	0.31 (.03)	0.22
^{87}Y	β^+cum	0.45 (.18)	–	0.51 (.21)	–
^{85}Sr	β^+cum	0.36 (.04)	0.38	0.46 (.05)	0.35
^{84}Rb	Indep.	0.27 (.04)	0.284	0.37 (.05)	0.204
^{83}Rb	β^+cum	0.345 (.035)	0.515	0.49 (.05)	0.41
^{75}Se	β^+cum	0.12 (0.02)	0.318	0.24 (.05)	0.21
^{74}As	Indep.	0.23 (0.02)	0.306	0.29 (.03)	0.25
^{72}Se	β^+cum	0.057 (0.015)	0.019	0.08 (.02)	0.03
^{65}Zn	β^+cum	0.084 (0.025)	0.209	0.18 (.06)	0.234
^{59}Fe	β^-cum	0.152 (.015)	0.224	0.160 (.015)	0.234
^{56}Co	EC cum.	0.007 (.003)	0.0156	0.019 (.007)	0.022
^{54}Mn	Indep.	0.086 (.013)	0.0312	0.073 (.012)	0.16
^{52}Mn	β^+cum	0.007 (.002)	0.047	0.022 (.006)	0.034
^{48}V	EC cum.	0.019 (.006)	0.069	0.033 (.010)	0.049
^{22}Na	β^+cum	0.087 (.017)	–	0.122 (.024)	–
^{7}Be	Indep.	0.33 (.06)	–	0.56 (.10)	–

Remark: For isomers, the total independent yield of the nuclide is given in the columns 4 and 6 without differentiation between isomeric and g.s. yields.

Table 2: **The same as Table 1, but taken at 423 MeV mean energy of protons**

Isotope	Type of yield	^{186}W target		^{nat}W target	
		Experiment	Calculation	Experiment	Calculation
^{184}Re	Indep.	6.1 (.3)	} 11.44	1.93 (.10)	} 4.55
^{184m}Re	Indep.	1.5 (.2)		0.50 (.08)	
^{183}Re	EC cum.	10.0 (1.5)	14.4	3.5 (.5)	8.0
^{183}Ta	β^- cum	23 (5)	–	14.0 (2.0)	–
^{182}Re	EC cum.	8 (2)	7.85	10 (3)	5.5
^{182}Ta	Indep.	18.2 (.9)	16.0	12.6 (.6)	15.8
^{181}Hf	β^- cum	2.5 (.3)	2.2	1.08 (.10)	1.17
^{179m2}Hf	Indep.	0.87 (.08)	3.4	0.39 (.04)	2.37
^{178}W	EC cum.	32.6 (3.3)	52.0	36.3 (3.6)	53.3
^{178m2}Hf	Indep.	0.52 (.10)	4.9	0.21 (.04)	3.4
^{177m}Lu	Indep.	0.26 (.06)	0.87	0.11 (.03)	0.38
^{175}Hf	EC cum.	78.0 (3.9)	78.3	79.5 (3.9)	77.5
^{174}Lu	Indep.	1.3 (.4)	} 2.7	1.2 (.4)	} 1.37
^{174m}Lu	Indep.	1.6 (.4)		1.4 (.4)	
^{173}Lu	EC cum.	76 (4)	76.5	78 (4)	77.3
^{172}Hf	EC cum.	69.0 (3.5)	63.9	78 (4)	70.8
^{171}Lu	EC cum.	77 (5)	66.9	85 (6)	73
^{169}Yb	EC cum.	62 (3)	55.3	69.0 (3.5)	60.9
^{168}Tm	Indep.	0.9 (.2)	0.6	0.6 (.1)	0.23
^{167}Tm	EC cum.	40 (2)	42.9	57.6 (3.1)	49.0
^{156}Tb	Indep.	0.33 (.06)	0.162	0.63 (.13)	0.17
^{156}Eu	β^- cum	0.10 (.03)	–	0.08 (.03)	–
^{155}Tb	EC cum.	10.8 (2.1)	7.16	12.4 (2.4)	10.5
^{151}Gd	EC cum.	1.84 (.22)	2.22	3.75 (.56)	3.83
^{149}Gd	EC cum.	1.58 (.24)	1.27	3.07 (.46)	2.42
^{149}Eu	EC cum.	1.59 (.24)	1.42	3.17 (.51)	2.60
^{148}Eu	Indep.	0.13 (.02)	0.206	0.15 (.02)	0.22
^{148m}Pm	Indep.	0.027 (.010)	0.006	0.025 (.008)	0.009
^{147}Eu	EC cum.	0.71 (0.7)	0.85	1.70 (.17)	1.76
^{146}Gd	EC cum.	0.61 (.06)	0.44	1.60 (.16)	1.18
^{145}Eu	EC cum.	0.29 (.05)	0.36	0.63 (.10)	0.88
^{144}Pm	Indep.	–	0.037	–	0.071
^{143}Pm	EC cum.	0.03 (.01)	0.247	0.12 (.04)	0.45

Table 2 (Continue)

Isotope	Type of yield	^{186}W target		^{nat}W target	
		Experiment	Calculation	Experiment	Calculation
^{140}Ba	β^-cum	0.0009 (.0004)	–	0.001 (.0004)	–
^{131}Ba	EC cum.	–	0.047	–	0.031
^{121}Te	EC cum.	–	0.053	–	0.037
^{113}Sn	EC cum.	0.027 (.009)	0.040	0.038 (.011)	0.037
^{110m}Ag	Indep.	0.039 (.008)	0.025	0.05 (.01)	0.017
^{106m}Ag	Indep.	0.052 (.010)	0.037	0.072 (.022)	0.04
^{105}Ag	EC cum.	0.15 (.03)	0.041	0.206 (.041)	0.052
^{103}Ru	β^-cum	0.12 (.04)	0.062	0.084 (.025)	0.028
^{102}Rh	Indep.	0.16 (.05)	0.056	0.089 (.030)	0.059
^{100}Pd	β^+cum	–	0.016	–	0.012
^{95m}Tc	Indep.	0.014 (.005)	–	0.012 (.004)	–
^{95}Nb	Indep.	0.15 (.02)	0.103	0.16 (.02)	0.08
^{95}Zr	β^-cum	0.063 (.007)	0.040	0.05 (.005)	0.027
^{91m}Nb	Indep.	0.024 (.008)	0.069	0.037 (.013)	0.08
^{88}Zr	EC cum.	0.087 (.009)	0.103	0.115 (.012)	0.154
^{88}Y	Indep.	0.194 (.020)	0.084	0.258 (.026)	0.09
^{87}Y	β^+cum	0.33 (.11)	–	–	–
^{85}Sr	β^+cum	0.24 (.02)	0.153	0.355 (.036)	0.117
^{84}Rb	Indep.	0.23 (.02)	0.103	0.312 (.031)	0.065
^{83}Rb	β^+cum	0.25 (.02)	0.190	0.36 (.036)	0.151
^{75}Se	β^+cum	0.08 (.02)	0.112	0.13 (.03)	0.059
^{74}As	Indep.	0.17 (.03)	0.078	0.245 (.040)	0.108
^{72}Se	β^+cum	0.03 (.01)	0.0125	0.05 (.02)	0.012
^{65}Zn	β^+cum	0.07 (.02)	0.084	0.08 (.03)	0.074
^{59}Fe	β^-cum	0.12 (.01)	0.109	0.141 (.014)	0.077
^{56}Co	EC cum.	0.011 (.004)	0.015	0.015 (.005)	0.0062
^{54}Mn	Indep.	0.064 (.021)	0.031	0.107 (.030)	0.043
^{52}Mn	β^+cum	0.005 (.002)	0.022	0.009 (.003)	0.015
^{48}V	EC cum.	0.007 (.001)	0.0125	0.012 (.002)	0.022
^{22}Na	β^+cum	0.086 (.009)	–	0.102 (.010)	–
^{7}Be	Indep.	0.29 (.03)	–	0.35 (.04)	–

Table 3: **The same as Table 1, but taken at 268 MeV mean energy of protons**

Isotope	Type of yield	^{186}W target		^{nat}W target	
		Experiment	Calculation	Experiment	Calculation
^{184}Re	Indep.	11.3 (.6)	} 19.4	3.35 (.17)	} 7.6
^{184m}Re	Indep.	2.6 (.4)		0.80 (.12)	
^{183}Re	EC cum.	13.0 (1.9)	24.5	5.7 (.9)	13.6
^{183}Ta	β^-cum	25 (5)	–	14.0 (2.8)	–
^{182}Re	EC cum.	16.0 (3.2)	13.2	–	9.7
^{182}Ta	Indep.	20 (1)	14.4	11.8 (0.6)	12.5
^{181}Hf	β^-cum	1.9 (.2)	1.4	0.82 (.08)	0.67
^{179m2}Hf	Indep.	0.72 (.07)	2.04	0.30 (.05)	2.37
^{178}W	EC cum.	56.8 (5.7)	78.9	54.6 (2.7)	79.8
^{178m2}Hf	Indep.	0.38 (.06)	3.0	0.17 (.04)	2.2
^{177m}Lu	Indep.	0.16 (.04)	0.44	0.08 (.03)	0.19
^{175}Hf	EC cum.	95.7 (4.8)	93.2	103.2 (5.2)	97.0
^{174}Lu	Indep.	1.2 (.3)	} 1.6	1.0 (.3)	} 0.82
^{174m}Lu	Indep.	1.1 (.4)		1.3 (.4)	
^{173}Lu	EC cum.	71.7 (4.2)	80.7	93.6 (4.8)	90.9
^{172}Hf	EC cum.	76.6 (3.5)	64.4	79.4 (3.5)	81.0
^{171}Lu	EC cum.	73.3 (4.8)	61	85.5 (4.5)	74.3
^{169}Yb	EC cum.	38.0 (2.1)	42.1	57.5 (2.8)	54.0
^{168}Tm	Indep.	0.32 (.08)	0.30	0.20 (.07)	0.105
^{167}Tm	EC cum.	18.0 (1.3)	26.0	36.4 (2.6)	37.3
^{156}Tb	Indep.	0.13 (.02)	0.03	0.18 (.06)	0.027
^{156}Eu	β^-cum	0.10 (.02)	–	0.09 (.03)	–
^{155}Tb	EC cum.	5.5 (1.1)	0.32	8.2 (1.6)	0.98
^{151}Gd	EC cum.	1.1 (.2)	0.017	0.95 (.2)	0.14
^{149}Gd	EC cum.	–	0.012	–	0.049
^{149}Eu	EC cum.	–	0.015	–	0.064
^{148}Eu	Indep.	0.03 (.01)	–	0.022 (.007)	0.003
^{148m}Pm	Indep.	0.012 (.004)	–	–	–
^{147}Eu	EC cum.	–	0.012	–	0.015
^{146}Gd	EC cum.	–	–	0.021 (.007)	0.023
^{145}Eu	EC cum.	–	0.0036	–	0.014
^{144}Pm	Indep.	–	0.0030	–	0.0062

Table 3 (Continue)

Isotope	Type of yield	^{186}W target		^{nat}W target	
		Experiment	Calculation	Experiment	Calculation
^{143}Pm	EC cum.	–	–	–	0.009
^{131}Ba	EC cum.	–	0.012	–	0.0062
^{121}Te	EC cum.	–	0.0062	–	0.022
^{113}Sn	EC cum.	0.007 (.002)	0.0062	0.019 (.005)	0.025
^{110m}Ag	Indep.	0.016 (.005)	0.003	0.014 (.005)	0.009
^{106m}Ag	Indep.	0.023 (.007)	0.016	0.023 (.007)	0.019
^{105}Ag	EC cum.	0.12 (.03)	0.012	0.19 (.05)	0.028
^{103}Ru	β^-cum	0.076 (.015)	0.0019	0.066 (.015)	0.012
^{102}Rh	Indep.	0.12 (.04)	0.016	0.11 (.04)	0.012
^{95m}Tc	Indep.	0.02 (.008)	–	0.020 (.009)	–
^{95}Nb	Indep.	0.10 (.01)	0.031	0.11 (.01)	0.03
^{95}Zr	β^-cum	0.058 (.006)	0.0094	0.060 (.006)	0.0054
^{91m}Nb	Indep.	0.04 (.01)	0.0062	–	0.037
^{88}Zr	EC cum.	0.050 (.005)	0.019	0.045 (.005)	0.019
^{88}Y	Indep.	0.085 (.009)	0.022	0.13 (.01)	0.03
^{87}Y	β^+cum	0.20 (.06)	–	0.24 (.07)	–
^{85}Sr	β^+cum	0.18 (.02)	0.022	0.20 (.02)	0.031
^{84}Rb	Indep.	0.127 (.013)	0.016	0.18 (.02)	0.012
^{83}Rb	β^+cum	0.10 (.01)	0.041	0.16 (.02)	0.065
^{75}Se	β^+cum	0.028 (.010)	0.016	0.06 (.02)	0.016
^{74}As	Indep.	0.059 (.012)	0.022	0.11 (.03)	0.009
^{72}Se	β^+cum	0.017 (.006)	–	0.028 (.010)	0.003
^{65}Zn	β^+cum	0.019 (.008)	0.019	0.027 (.010)	0.0123
^{59}Fe	β^-cum	0.052 (.005)	0.044	0.069 (.007)	0.028
^{56}Co	EC cum.	0.010 (.003)	–	0.015 (.005)	0.006
^{54}Mn	Indep.	0.040 (.012)	0.006	0.044 (.014)	0.022
^{52}Mn	β^+cum	0.006 (.002)	0.006	0.006 (.002)	0.006
^{48}V	EC cum.	0.008 (.002)	–	0.008 (.002)	–
^{22}Na	β^+cum	0.06 (.01)	–	0.05 (.01)	–
^{7}Be	Indep.	0.17 (.03)	–	0.15 (.03)	–

Looking the tables, one may conclude that general behavior of the product mass-distribution is similar both for ^{nat}W and ^{186}W targets. Despite that, the enriched ^{186}W target is (2.5–3) times more productive as compared to the ^{nat}W

one for the accumulation of the high-spin isomers of Hf and Lu. Significant discrepancy for the yields of A > 180 products is understood, because of a different isotopic composition of both targets.

Comparison of the measured and calculated cross sections shows again schematical similarity, but the deviations are also visible for some individual products, in particular, for β^- radioactive products of spallation. Light ^{22}Na and ^{7}Be nuclides have been observed, and the expected growth of the fragmentation yield at A < 30 is experimentally confirmed. In principle, light products can be formed due to an admixture of light stable elements in the target assembling. But in the present work, the ^{22}Na and ^{7}Be yields are found comparable at the cases of both pure metal $^{\rm nat}$W and isotopically separated targets. This makes evident their origin from the fragmentation of the W nuclei. The ^{52}Mn, ^{56}Co and ^{72}Se products have been systematically detected, and their low yields do not contradict the calculations at 630 MeV. The ^{60}Co γ lines are found at right energies, but the relative intensity and decay factors are inconsistent and disturb the successful identification. There is, obviously, the admixture of other isotopes activity. More details on the product distributions are given below.

2. MASS DISTRIBUTION AND FISSION-TO-SPALLATION RATIO

The results of Tables 1–3 can be plotted in a form of mass-distribution covering both the spallation and fission-fragment mass-ranges. In Fig. 2, the results for $^{\rm nat}$W and ^{186}W targets at beam energy of 650 MeV are shown. For the comparison, mass distributions taken with $^{\rm nat}$Ta and $^{\rm nat}$Re targets in Refs. [1, 9] are also reduced at the same beam energy in Fig. 3. Regular behavior of the points and similar character of distributions for all 4 targets confirm the reliability of the applied method for the mass-distribution measurement. Some comments are needed for understanding the idea of method.

Neutron deficient nuclides are produced with highest probability in the spallation reaction, and they are decayed via β^+ and EC-decay modes to long-lived isobars past cooling time. Such cumulative isobaric nuclides serve as a trap for the mass-yield of a given mass A. Thus, the measured cumulative yields allow constructing the mass-distribution of the spallation products. We used this method and, as shown in Fig. 2, it results in a very regular mass dependence. The scattering of points is within standard errors confirming the reliability of the results for the spallation products.

However, the information about the charge distribution for a given A is lost this way. It is difficult to apply the activation method for the measurement of independent yields of many isobaric nuclides even when the short-time cycle of irradiation detection is provided, as in Ref. [6]. Results [6] demonstrate at some cases a consequence of cross sections for a few isotopes at fixed Z-number, but

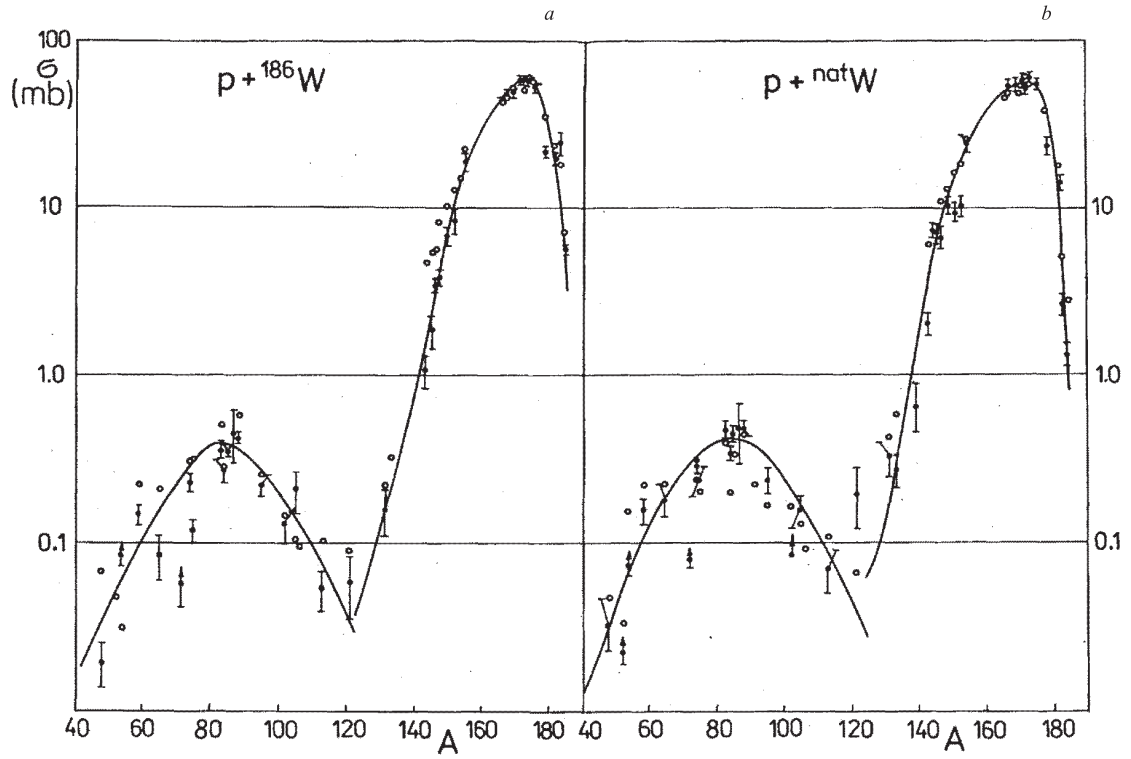

Fig. 2. Mass-distributions of the nuclides produced in the ^{186}W (*a*) and ^{nat}W (*b*) targets exposed to protons at mean energy of 630 MeV. Experimental results are shown as black circle with error bars while the ones calculated with LAHET are shown as opened circles. The lines are only to guide the eyes

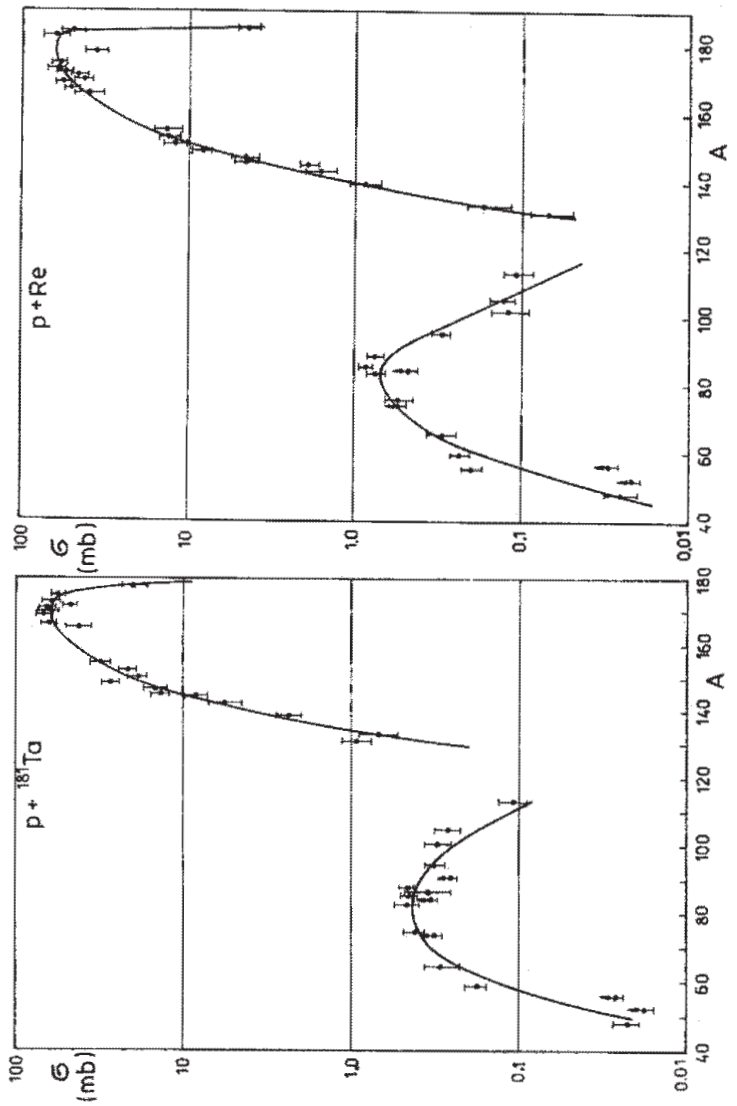

Fig. 3. The same as Fig. 2, but taken with $^{\mathrm{nat}}$Ta and $^{\mathrm{nat}}$Re targets

not isobars at fixed A-member. Moreover, some isotopes are produced independently, while others due to the accumulation of isobaric-chain yields and, thus, the construction of regular isotopic distribution of independent yields is impossible. At the best cases, 3–4 independent yields of the same-element isotopes can be measured, and this is not enough for deducing a regular dependence. Even worse situation takes place for the isobaric Z-distribution, because the information is needed about nuclides having lifetimes in the range of seconds. The direct instrumental separation of fragments in inversed kinematics experiments would be more appropriate for (Z, A)-distribution measurements but such experiments can be conducted only with the heavy-element ions accelerated up to energies in the range of 1 GeV/u. Such experiments are described in Refs. [10, 11].

Mass distributions in Figs. 2 and 3 are plotted using cumulative yields of the fragmentation products. Points correspond to some individual A numbers that are characterized by the convenient properties of the isobaric chain of nuclides. The trapping of a total yield to the longer-lived isobar is a necessary requirement, and in addition, this isobar should be easily determined by the gamma-spectra measurements. Hence, a mass-yield value can be determined only for some special mass-numbers. Despite blank intervals between points, they show regular behavior in Figs. 2, 3, especially near the maximum of mass-distribution. Important peculiarity is a presence of two peaks belonged to the spallation and fission mechanisms of the reaction. One may expect that our mass-distribution would be poor as compared to the Refs. [5, 6] because short-lived products were accessible at measurements [5, 6]. But in practice, the comparable number of points has been successfully determined in our case, as well. This is because low-activity products can be detected after one-month cooling time, and the additional group of nuclides is involved in the mass-dependence of yields.

A wide peak centered on $A \approx 85$ corresponds to the fission fragments. Fission mass yields have also been determined by the cumulative products with addition in some case the independent isobar yields. The curves in Fig. 2, 3 for fission peak are drawn through points, averaging the noticeable scattering of points. Larger scattering than for the spallation products is, in part, due to the lower yields and correspondingly higher random errors and, in part, due to the incomplete cumulativity of some yields. The line of most probable charge $Z_P(A)$ for fission fragments is located not far from the β-stability line, and a coefficient of cumulativity depends on the individual properties of the isobaric chain. For many mass-numbers, above 70% of the mass-yield is collected by cumulative product, but in some cases the cumulativity is clearly incomplete. Such points have been selected and excluded or shown as lower limits in Figs. 2, 3.

The scattering of points is obviously most important source of the inaccuracy in estimation of the fission-to-spallation ratio. The spallation and fission peaks have been integrated over corresponding mass ranges and total spallation (σ_s) and fission (σ_f) product cross sections have been deduced. The curves

shown in Figs. 2 and 3, are used for interpolations and extrapolations, and the inaccuracy is partially reduced by such smoothing procedure. The decomposition of two processes near A = 120 makes no difficulties. The Gaussian fit has not been applied because the spallation peak has definitely another shape, and fission symmetric maximum also can be distorted by other processes. The ternary and multifragmentation yields may be superimposed with the binary fission yield at the mass range of $A \leqslant 80$. The role of multifragmentation was stressed in Ref. [12]. But yet, the probability of binary fission dominates strongly over that of more complicated processes, like ternary fission or multifragmentation.

A sum of individual mass cross sections for fission peak produces the double total cross section of fission: $2\sigma_f$. A factor of 2 is just because two fragments arise at one fission event. Thus, we assume here that the contribution of multiple processes is negligible, and the fission peak corresponds exclusively to the binary fission. An indirect confirmation of that can be found in the fission peak width. For Ta, mass distribution looks a little wider than for Re target. Such variation could be expected because of Z^2/A parameter of the fissile nucleus changes. This is, obviously, manifested in the experimental results. Integrating over the fission and spallation peaks, one deduced the total fission-to-spallation ratio within an accuracy of about 20%. Similar accuracy was achieved in Refs. [10, 13] for Au and Pb targets applying other methods.

In Fig. 4, the fission-to-spallation ratio $(2\sigma_f/\sigma_s)$ is shown versus proton-beam energy for ^{186}W, Ta and Re targets and versus Z^2/A parameter including the literature results [10, 13] for Au and Pb targets. Two latter points are taken at 800 MeV (not at 650 MeV), but this inconsistency does not disturb a general conclusion that the fission probability is strongly increased with Z^2/A growth. The energy dependence is much weaker at the range of $E_p > 600$ MeV. The points in Fig. 4 correspond to Z^2/A parameter calculated for a compound nucleus. Actually, the fissile nucleus is formed as a spallation residue after emission of many neutrons and protons. The compound-nuclei Z^2/A values still reflect the variation of mean Z^2/A parameter with changing the targets, and may serve in Fig. 4 as a relative scale.

Let us discuss now the comparison of measured and calculated yields of the fragmentation product. The LAHET code had been adjusted for use it in previous studies during past years, in particular, at the investigation of fragmentation of exotic radioactive targets: of ^{241}Am [14] and ^{129}I [15]. Presently, tungsten fragmentation yields are simulated for individual products and they have been shown in Fig. 2. One can notice the general good agreement between the theory and experimental results, and it is remarkably good near the maximum of the spallation products distribution.

The total yield of the spallation reaction as well as the yields for the cumulative products can be reproduced. This is clearly seen in Fig. 5 where calculated excitation functions are shown for the most probable products of the ^{186}W spal-

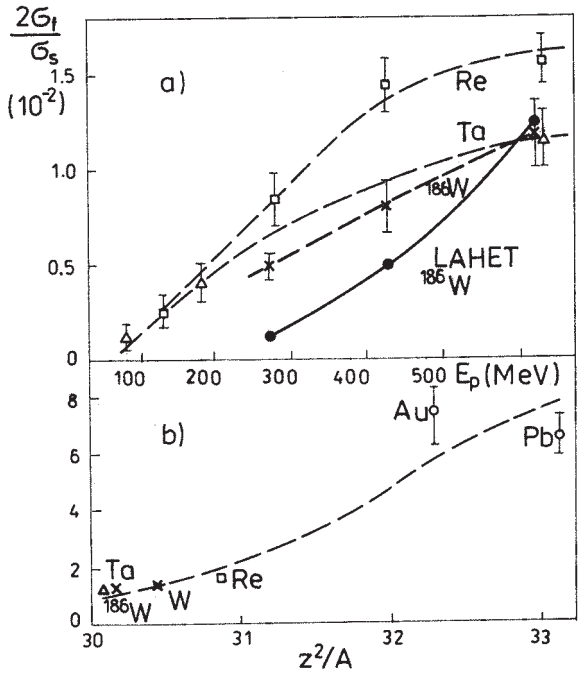

Fig. 4. Fission-to-spallation ratio plotted versus a) the mean proton energy for Ta, ^{186}W and Re targets and b) versus Z^2/A parameter of the compound nucleus. Points corresponding to the measurements of Refs. [10, 13] for Au and Pb targets are added. Curves are the guide lines. Simulation results for ^{186}W are given as points without error bars

lation. These nuclides contribute a significant fraction to the total activity of the exposed target past 30 days cooling. The experimentally determined yields are also given in Fig. 5, and they show good agreement with the theory, except the yield of ^{178}W that is systematically lower the predicted one. The statistical accuracy is rather good for ^{178}W both in the experiment and in the simulation. Systematical deviation may mean that the tabular values of the quantum yield for the ^{178}W γ-lines are a little overestimated (by 20–30%). Unfortunately, new updated spectroscopical parameters are not yet available for ^{178}W. The similar situation took place earlier at the case of ^{173}Lu, when the quantum yields were used according Ref. [3]. Later, improved values taken from "Nuclear Data Sheets" led to the exclusion of the discrepancy.

The independent production yields are given in Fig. 5 for the ^{179}Hf, ^{178}Hf and ^{177}Lu nuclides. They are needed for the estimation of the isomer-to-ground state ratio when the yields of the isomeric state are successfully measured. For these

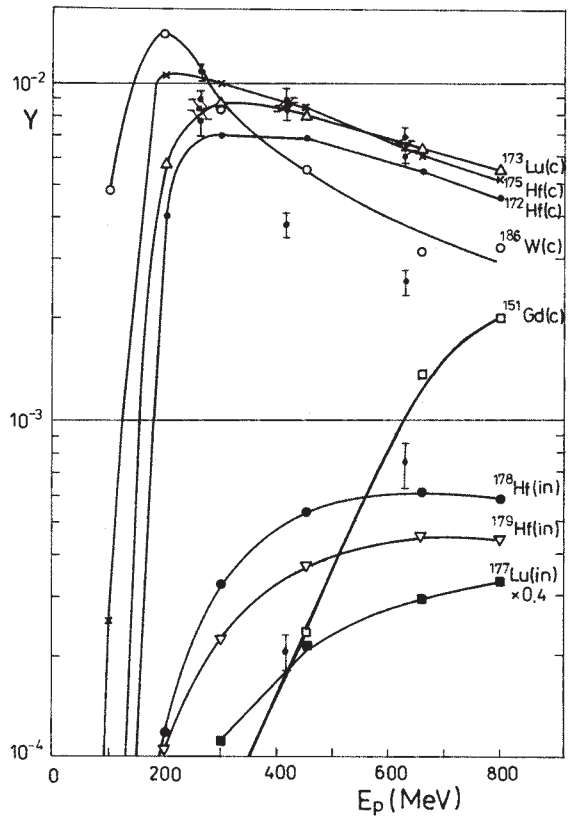

Fig. 5. Excitation functions of independent and cumulative yields for the spallation products as predicted by the LAHET code simulation for the p+^{186}W reaction. Measured cumulative yields are shown as small points with error bars. Curves are the guide lines

β-stable or even neutron-rich isotopes, the predictions have not been confirmed in measurements. ^{177}Lu has been observed but with poor statistics. Some other β^- active nuclides, for instance, ^{156}Eu and ^{140}Ba are systematically manifested in the measurements, despite their low yield. At the same time, they never appear in the simulations at all. This may be explained as following: the yield of β^- active nuclides corresponds to tail of the isotopic distribution, and the yield of products far from the most probable isotopes is not well reproduced.

In the simulation for masses A $\leqslant$ 120, the yields of individual fission products are evaluated and compared to the experimental values. As mentioned above, the incomplete cumulative factor produces a larger dispersion of the points. Even so, the simulated trend of the mass-distribution looks rather similar to the experimen-

tal one. The total yield of the fission is rather well reproduced in the simulation at 630 MeV, but the discrepancy increases for lower incident proton energies, as is clear from Fig. 4.

A strong increase of the fission-to-spallation ratio with Z^2/A (see in Fig. 4) looks absolutely natural because the fission probability is determined by the fission barrier value, which depends on the fissility parameter Z^2/A. Unexpectedly, the energy dependence is not reproduced by the simulations, not even the trend of the function. The reason could be the omission in the LAHET calculations of the spallation residues angular momentum. In the code, the first stages of the reaction are described using the models of intra-nuclear cascade and pre-equilibrium emission. The residual nucleus (Z, A) and its excitation energy are among the controlled physical variables but not its angular momentum. At the same time, the fission probability is very sensitive to the angular momentum and consideration of the angular momentum can improve the agreement between theory and experiment in Fig. 4. The angular momentum of the residual nucleus is important also because it plays a key role in the production of the high-spin isomers. Strictly speaking, the calculation of the fission probability contains many parameters that are not yet well defined at independent experimental calibrations. Thus, there is some freedom for parameter variations to improve the agreement with the measured fission-to-spallation ratio. Even so, the production of high-spin isomers with relatively high yields may indicate that the spallation residues possess significant angular momentum and it has to influence the fission probability.

3. PRODUCTION OF ISOMERS

Production of high-spin isomers in reactions with the intermediate-energy protons has started to be an object of extensive studies during past few years. In Refs. [16, 17] and in other articles by this group, the isomers were observed in the reactions induced by the intermediate-energy heavy ions. In Ref. [18], the isomeric yields were measured for the medium atomic-mass targets with proton beam. However, the isomers at the range near A = 180 are of special interest because they are characterized by unique combination of the high excitation energy with high spin and K-quantum numbers and with long lifetime. Such properties are optimal in the sense of the isomer application for the storage of energy. Spallation yields of the long-lived high-spin isomers of ^{179m}Hf, ^{178m2}Hf and ^{177m}Lu are quantitatively determined in Ref. [1] after measurements of the Ta and Re targets activation with protons at the 100–650 MeV energy range. Later, similar results appeared also in Refs. [5, 6], but not for the most interesting ^{178m2}Hf isomer that was successfully detected and measured only in Ref. [1], because it has long half-life, $T_{1/2} = 31$ years, and rather low specific activity, respectively.

The present studies are the continuation of this series of measurements for the ^{nat}W and 97% enriched ^{186}W targets. It was expected that ^{186}W can be the best stable target for the production of mentioned long-lived isomers. And it was really confirmed after the measurements described above. We are concentrating now on the discussion of the ^{179m2}Hf, ^{178m2}Hf and ^{177m}Lu isomer yields, despite in Tables 1–3 one can see also the cross sections for ^{184m}Re, ^{174m}Lu, ^{110m}Ag, ^{106m}Ag, ^{95m}Tc and ^{91m}Nb. All of them should be discussed elsewhere, for instance, in the context of the fission-fragment angular momentum for the latter 4 isomers.

The experimental results in Tables 1–3 contain the isomeric yield and cross section values, while calculations give only the total yield without distinguishing between the isomer and ground-state yields. At the same time, the experimental results were also incomplete, because the ground-state and total yields could not be measured for stable isotopes by the activation technique. Finally, the combination of both experimental and simulated cross sections allows one to complete the results and determine the isomer-to-ground state ratio σ_m/σ_g. The cross section and σ_m/σ_g values are compared in Table 4 for the production of isomers with 650 MeV proton beam using different targets. The highest-activity neighboring radionuclides are also characterized in Table 4, because they define the radioactive contaminations in the produced isomeric material. This is clear that background isotopes are produced with very similar cross sections when different targets are used. However, the productivity for isomers varies strongly. As expected, the best would be a ^{186}W target, its application leads to the increase of the cross section by a factor of about 2.5 for high-spin isomers of Hf and Lu. This takes place not only at 650 MeV of the beam energy, but at 450 MeV, as well.

The cross section values reduced in Table 4 can be directly used for the calculation of the number of produced isomeric atoms and contaminating nuclides at some irradiation. Higher cross section is resulted immediately in a shorter time of the irradiation, needed to accumulate the same quantity of the isomer matter.

The isomer-to-ground state ratios are given in Table 4, and these results would be significant for the physical conclusion by the nuclear-reaction mechanism. Unfortunately, the estimation of σ_m/σ_g value is somewhat model dependent, because we need to use the calculated σ_g values for stable ground-state nuclei. However, as discussed above, the LAHET code simulations describe well the yield of many radioactive products, in particular, at the range of A = 170–180. Thus, the estimated σ_m/σ_g values should be reliable, at least, within a deviation of about $\pm$40%. This is enough to make some conclusion. Indeed, the σ_m/σ_g values of the order of 10–20% in magnitude are higher known in literature for the production of the high-spin isomers at other producer reaction. Respectively, the spallation residue angular momentum, should not be low, probably as high as 10 $\hbar$, or even higher. The dependence of σ_m/σ_g value from the target mass-

number indicates the increase of the residual spin with the growth of the number of emitted nucleons. For instance, the total ^{178}Hf cross section decreases from Ta to Re, while σ_m/σ_g is, on the contrary, increasing. With ^{186}W target, the total cross section for ^{179}Hf, ^{178}Hf and ^{177}Lu nuclides formation is higher than with Re, while σ_m/σ_g is much better than with Ta. Thus, ^{186}W is the best target, because both σ_m/σ_g and total cross section $(\sigma_m + \sigma_g)$ for the nuclides production are optimal at this case.

Table 4: **Cross sections and isomer-to-ground state ratios for the formation of high-spin isomers after spallation of different targets at proton beam energy of 650 MeV. The highest activity products are also listed for the comparison**

Nuclide	Target			
	^{nat}Ta	^{nat}W	^{186}W	^{nat}Re
	Cross section σ (mb)			
^{179m2}Hf	0.52	0.36	0.80	0.12
^{178m2}Hf	0.31	0.18	0.48	0.13
^{177m}Lu	0.15	0.13	0.26	0.04
^{178}W	5.9	23	21.8	36
^{175}Hf	56	55	55.6	59
^{172}Hf	47	53.5	57.4	55
^{173}Lu	61	61	60	61
	σ_m/σ_g ratio			
^{179m2}Hf	0.040	0.14	0.25	0.24
^{178m2}Hf	0.021	0.044	0.092	0.14
^{177m}Lu	0.103	0.21	0.29	0.40

Remark: Errors for the cross section values are given in Table 1, and for the σ_m/σ_g ratio, possible systematic errors must be added because σ_g is taken from the simulation.

This way, it becomes also understood, why cross sections for isomers are much lower the cumulative cross section for the corresponding A number. The independent yield of some β-stable nuclide is a little fraction of the isobaric-chain integrated yield, then it is additionally suppressed because of $\sigma_m/(\sigma_m + \sigma_g) < 1$.

Mean angular momentum of the spallation residue deduced from the σ_m/σ_g values correlates well with the conclusion described above after analysis of the fission-to-spallation ratios. Both confirm a reasonably high momentum that influences significantly the probability of fission and the yield of isomers.

4. SUMMARY

The series of experiments have been carried out at Dubna synchrocyclotron for the measurement of the fragmentation-products cross sections with tungsten targets at proton energies of 300–650 MeV. The developed method demonstrates that high sensitivity measurements can be arranged with the enriched ^{186}W target using rather modest amount of the expensive isotope. The yield of as many as of about 70 radionuclides have been successfully observed and quantitatively determined. Among them, 9 isomers are successfully detected. The mass-distribution of the fragmentation products can be constructed and then the relative yield of the spallation and fission reactions is deduced. Experimental values are systematically compared with the results of Monte-Carlo simulations using the LAHET code. The fission probability is, obviously, influenced due to a reasonably high angular momentum of the spallation residue. This conclusion is then confirmed after the estimation of isomer-to-ground state ratios.

For the high-spin isomers of ^{179m2}Hf, ^{178m2}Hf and ^{177m}Lu, the enriched ^{186}W target provides the significant gain in a productivity of about 2.5 times higher as compared to the target of natural isotopic composition $^{\mathrm{nat}}$W. The isomer-to-ground state ratios are estimated as a result of measurements, and they contribute an important addition to rather pure set of known values for the spallation reactions.

At practical application, a factor of 2 or 3 in productivity (cross section) means just 2–3 times lower expenses for the accumulation of the same amount of isometric material in extensive irradiations at intermediate energy proton accelerators.

ACKNOWLEDGMENTS

This work was supported by the US Air Force European Office of Aerospace Research and Development, London via IGE Foundation, Bucharest.

REFERENCES

1. S.A. Karamian, J. Adam, D.V. Filossofov, et al., Nucl. Instr. Meth., A489 (2002) 448.

2. R.B. Firestone and V.S. Shirley. Table of Isotopes, Eight Edition, Wiley, New York, 1996.

3. N. Reus and W. Westmeier. At. Data Nucl. Data Tables, 29 (1983) 1.

4. H. Schopper (Ed.). Production of Radionuclides at Intermediate Energies, Springer, Berlin, 1993, subvolume C.

5. B.L. Zhuikov, M.V. Mebel, V.M. Kokhanyuk, et al., Phys. Rev. C68 (2003) 054611.

6. Yu.E. Titarenko, V.F. Batyaev, E.I. Karpikhin, et al., IAEA Nucl. Data, http: www-nds.iaea.org/indc_sel.html

7. J. Adam, J. Mrázek, J. Frana, et al., Measurement Techniques 44 (2001) 93.

8. R.E. Prael and H.Lichtenstein, LANL Report LA-UR-89-3014, 1989, Los Alamos; http: // www-xdiv.lanl.gov/XTM/lcs/lahet-doc.html.

9. S.A. Karamian and J. Adam, Czechoslovak. J. Phys. 53, Suppl. A (2003).

10. J. Benlliure, P. Armbruster, M. Bernas, et al., Nucl. Phys. A683 (2001) 513.

11. J. Benlliure, P. Armbruster, M. Bernas, et al., Nucl. Phys. A700 (2002) 469.

12. Yu.A. Chestnov and B.U. Sokolovsky, Yadernaya Fizika, 64 (2001) 1541.

13. Yu.E. Titarenko, O.V. Shvedov, M.M. Igumnov, et al., Nucl. Instr. Meth., A414 (1998) 73.

14. J. Adam, A. Balabekyan, R. Brandt, et al., Yadernaya Fizika, 65 (2002) 797.

15. J. Adam, A. Balabekyan, R. Brandt, et al., J. Nucl. Sci. and Technol., Suppl. 2 (2002) 272.

16. R. Grzywacz, R. Anne, G. Auger, et al., Phys. Rev. C55 (1997) 1126.

17. M. Pfützner, P.H. Regan, P.M. Walker, et al., Phys. Rev. C65 (2002) 064604.

18. V.M. Alexandryan, G.S. Ivazyan, A.R. Balabekyan, et al., Yadernaya Fizika, 59 (1996) 592.

Received on January 27, 2004.

Корректор *Т. Е. Попеко*

Подписано в печать 10.03.2004.
Формат 60 × 90/16. Бумага офсетная. Печать офсетная.
Усл. печ. л. 1,68. Уч.-изд. л. 2,12. Тираж 310 экз. Заказ № 54311.

Издательский отдел Объединенного института ядерных исследований
141980, г. Дубна, Московская обл., ул. Жолио-Кюри, 6.
E-mail: publish@pds.jinr.ru
www.jinr.ru/publish/